Talin1 Promotes Prostate Cancer Invasion and Metastasis via AKT Signaling and Anoikis Resistance

Shinichi Sakamoto[1], Richard O. McCann[2], and Natasha Kyprianou[1, 3, 4]

Departments of [1]Surgery/Urology and [3]Molecular & Cellular Biochemistry, and [4]Markey Cancer Center, University of Kentucky College of Medicine, Lexington, KY. [2]Mercer University School of Medicine, Division of Basic Medical Sciences, Macon, GA.

Address correspondence to:

Dr. Natasha Kyprianou

Division of Urology, MS-283

University of Kentucky Medical Center

800 Rose Street

Lexington, KY 40536

Telephone: 859-323-9812/**Fax:** 859-323-1944

E-mail: nkypr2@uky.edu

Key Words: Prostate cancer, Talin, Anoikis, Metastasis, Foal adhesions, Integrins, AKT

Running Title: Role of Talin1 in Prostate Cancer Metastasis

Support: This work was supported by an NIH R01 CA107575-06 grant (NK), a Markey Cancer Foundation Grant (NK). Shinichi Sakamoto is an American Urological Association Foundation Research Scholar.

Abbreviations: ECM; extracellular matrix, ILK-1; integrin linked-kinase 1, GSK3b; Glycogen synthase kinase 3 beta, MAPK; mitogen activated protein kinase, FAK; focal adhesion kinase, TRAMP; transgenic adenocarcinoma of the mouse prostate, BSA; bovine serum albumin, SDS-PAGE; sodium dodecyl sulfate polyacrylamide gel electrophoresis, pEGFP; red-shifted variant of wild-type Green fluorescence protein, DAPI; 4',6-diamidino-2-phenylindole, poly-HEMA; poly (2-hydroxyethyl) methacrylate, TBST; TRIS buffered saline with Tween 20, BPH; Benign Prostate Hyperplasia

ABSTRACT

Talin1 is an integrin regulatory protein that mediates integrin interactions with the extracellular matrix (ECM). This study investigated the significance of talin1 in prostate cancer progression to metastasis *in vitro* and *in vivo.* Talin1 overexpression enhanced prostate cancer cell adhesion, migration and invasion by activating survival signals and anoikis resistance. ShRNA-mediated talin1 loss led to a significant suppression of prostate cancer cell migration and transendothelial invasion *in vitro* and a significant inhibition of prostate cancer metastasis *in vivo.* Talin1 regulates cell survival signals via phosphorylation of focal adhesion kinase (FAK) and AKT. Targeting AKT activation led to a significant reduction of talin1-mediated prostate cancer cell invasion. Furthermore, talin1 expression was determined by immunostaining in prostate tissue from the TRAMP mouse model and in human prostate cancer specimens. Talin1 levels directly correlated with prostate tumor progression to metastasis in TRAMP mice. Talin1 profiling in human prostate specimens revealed a significantly higher expression of cytoplasmic talin1 in metastatic tissue compared to primary prostate tumors and benign prostate tissue ($P<0.0001$). This evidence suggests a potential value for talin1 as a marker of prostate cancer metastasis and implies that disrupting talin1 mediated signaling may have therapeutic significance in the treatment of metastatic disease.

INTRODUCTION

Cancer metastasis is a multistep and complex process that involves dissociation of the tumor cells from the organ of origin, degradation of the extracellular matrix (ECM), cell migration, anchorage-independent growth, apoptosis evasion, angiogenesis, invasion of surrounding tissues, cell adhesion, movement and colonization to distant sites in the body[1]. Human prostate cancer progression to advanced metastatic disease is associated with relapse to a hormone-refractory state due to impaired apoptotic response to androgen ablation. Androgen-independent prostate cancer cells become resistant due to roadblocks in apoptosis and depending on the interactions with the tumor microenvironment, acquire invasive and metastatic properties[2]. Both tumor epithelial and endothelial cells require attachment to the ECM for survival; commonly upon loss of adhesion, cells undergo detachment-induced cell death, or anoikis. Anoikis, a unique phenomenon of apoptosis consequential to insufficient cell-matrix interactions[3,4], is recognized as a significant player in tumor angiogenesis and metastasis[5]. During metastatic progression, cells are in a dynamic state lacking firm attachment to the ECM and susceptible to anoikis[5]. Resistance to die via anoikis dictates tumor cell survival and provides a molecular basis for therapeutic targeting of metastatic prostate cancer. Integrin-linked kinase (ILK) has been recognized as contributor to anoikis resistance via its ability to regulate several integrin-mediated cellular processes including cell adhesion, fibronectin-ECM assembly and anchorage-dependent cell growth[6-8].

Integrins are cell membrane receptors that mediate the functional interactions between a cell and the ECM, thus serving as bidirectional transducers of extracellular and

intracellular signals, ultimately regulating adhesion, proliferation, anoikis, survival and tumor progression[9-12]. Talin1 is a cytoskeletal linker protein that interacts with the cytoplasmic domain of integrins leading to integrin activation[10,13] and regulates their adhesion to extracellular ligands[14]. Talin1-deficient mice exhibit failure of integrins to aggregate into clusters and connect to the cytoskeleton, resembling the integrin deficient phenotype, and supporting that integrin function is talin1-dependent[15]. Furthermore recent studies in *Drosophila*, demonstrate that talin1 suppresses E-cadherin expression independent of integrin[16], indicating a role for talin1 distinct from the integrin-dependent mechanism. The contribution of talin1 to cancer development and progression has not previously investigated.

The present study investigated the role of talin1 in prostate cancer progression to metastasis. Our results indicate that talin1 engages the PI3-K/AKT signaling as the intracellular survival mechanism to confer anoikis resistance and promote invasion of human prostate cancer cells. Moreover, talin1 profiling in human prostate cancer specimens revealed a significantly increase in talin1 expression in metastatic prostate compared to benign and primary prostate tumors.

RESULTS

The effect of talin1 overexpression on the adhesion ability and migration potential of prostate cancer cells were first examined *in vitro*. GFP-talin1 stable transfectants of human PC-3 prostate cancer cells were generated, since this cell line expressed very low endogenous talin1 levels (Fig. 1A, and Sup1). Overexpression of talin1 significantly increased both the adhesion (Fig. 1B) and migration potential of prostate cancer cells compared to vector control cells (Fig. 1, panels C, D). We subsequently determined the consequences of talin1-overexpression on the invasion potential of prostate cancer cells through an endothelial cell monolayer. The trans-endothelial migration (TEM) assay was performed using the human brain membrane endothelial cells (HBMEC). Talin1 overexpression led to a significantly increased prostate cancer cell invasion through endothelial cell monolayer (Fig. 1, panels E and F).

Prostate tumor epithelial cell survival requires continuous attachment to the ECM and it is recognized that fibronectin, laminin and collagen participate in the formation of attachment plagues linked to the actin cytoskeleton. The impact of talin1 loss on prostate cancer cell adhesion was examined by generating ShRNA-talin1 stable transfectants in DU-145 prostate cancer cells that are characterized by high endogenous talin1 expression (Sup. 1). As shown on Fig 2A, ShRNA silencing of talin1 effectively reduced talin1 expression in DU-145 cells (>80%). Talin1 silenced DU-145 cells exhibited a reduced ability to adhere to different ECM components including collagen, laminin and fibronectin (Fig. 2B). Furthermore loss of talin1 led to significant reduction in the migration potential compared to vector control cells (Fig. 2, panels C and D).

Examination of the invasion ability of talin1-silenced transfectants through an endothelial cell monolayer revealed a significant suppression (Fig. 2, panels E and F).

The mechanism via which talin1 activates intracellular signals was subsequently examined in the context ECM-epithelial cell interaction. We focused on the FAK/AKT and the intracellular MAP kinase signaling pathway, as both mechanisms have been implicated in integrin-focal adhesion dependent signals[17]. Activation of FAK due to phosphorylation (Y397) was observed on collagen attachment conditions, while it was more prominent on fibronectin coated ECM in talin1 overexpressing cells relative to control cells (Fig. 3A). Talin1 overexpression also resulted in a marked activation on phosphorylation of AKT (Ser473) under fibronectin-attachment conditions, while only a modest activation of p44/42 MAP kinase was observed (Fig. 3A). The expression level of integrin-dependent signals was confirmed by confocal microscopy (Fig. 3B). Talin1 overexpressing cells exhibited increased expression of P-FAK, P-AKT and P-MAPK proteins relative to vector control cells upon fibronectin-aatachment conditions (Fig. 3B). Furthermore, talin1 overexpression enhanced AKT phosphorylation within the first 3hrs of incubation (Fig. 3, panels C, D), an change that temporally preceded a significant increase in phosphorylated FAK and MAPK (Fig. 3C, D).

The effect of talin1 on integrin-focal adhesion complex signaling interactions was subsequently investigated, by examining the direct binding of talin1 to integrn β3, a key talin1 binding partner [18]. To this end we used the DU-145 cell line, which exhibits high endogenous expression of integrin β3 (data not shown). Talin1 silencing significantly reduced the protein binding to integrin β3, as well as the focal adhesion partners, FAK and SRC (Fig. 3E). The reduced binding of SRC upon talin1 loss, led us

to determine the role of ILK-1, a protein that regulates SRC binding in response to integrin activation (Fig. 3F). Immunoprecipitation by integrin β3 revealed a significant decrease in ILK-1 interaction in talin1-silenced prostate cancer cells. Immunoprecipitation by ILK-1 also revealed a similar pattern, indicating that talin1 loss inhibited ILK-1 binding to integrin β3 complex (Fig. 3F).

In view of the emerging role of anoikis resistance as a critical contributor to metastasis during cancer progression[5], we subsequently examined the impact of talin1 overexpression on cell viability under ECM independent cell-suspension conditions, characteristic of anoikis. After plating on either fibronectin-coated matrix or the nonadhesive polyhydroxyethylmethacrylate (poly-HEMA), cells undergoing apoptosis were detected using the Annexin V staining. As shown on Figure 4A, talin1 did not exert a significant apoptotic effect under adherent conditions; however, in cell-suspension conditions, talin1 overexpressing prostate cells exhibited a significantly reduced apoptosis (Fig. 4A). Moreover, talin1 overexpressing cells exhibited an activation of FAK (Y397), AKT (Ser473) and SRC, but the response was weaker compared to the one obtained under fibronectin conditions (Fig. 4B). A modest activation of p42/44 MAPK was also observed in talin1 overexpressing cells. A time-course analysis of the anchorage independent phosphorylation of these proteins revealed a significant increase in phosphorylation of FAK, AKT and SRC in talin1-overexpressing cells within 6-24hrs (Fig. 4, panels C and D). Since ILK-1 mediated signaling is involved in anoikis resistance[19,20], we subsequently examined the phosphorylation of GSK3-b as a direct down stream signals of ILK-1. As shown in Fig. 4, there is an increased phosphorylation

of GSK-3b in non-adherent conditions in talin1 overexrpessing cells that was temporally associated with reduced amount of cleaved caspase-3 (Fig.4, panels E and F).

To determine whether AKT activation is an integral part of talin1 intracellular signaling, the consequences of AKT inhibition on talin1-mediated biological effects were examined. Since AKT activation comprises a critical signaling effector in anoikis resistance[21] we next studied the impact of talin1 overexpression on anoikis. The data on Figure 5A indicate that inhibiting AKT had no significant effect on the adhesion potential of GFP-talin1 prostate cancer cells on neither fibronectin nor laminin-coated matrix. In the presence of the AKT inhibitor, a significant suppression of both the migration potential (Fig. 5, panels B, C) and invasion ability (Fig. 5, panels D and E) was detected in talin1 overexpressing prostate cancer cells ($P<0.01$).

Resistance to anoikis is being recognized as a potentially important mechanism underlying tumor cell metastatic dissemination[5]; thus in subsequent experiments we pursued the functional characterization of talin1 in determining the metastatic potential of prostate cancer cells *in vivo.* Talin1 loss in prostate cancer cells led to a significantly reduced number of metastatic tumor lesions to the lungs compared to control cells (Fig. 6A). The significance of talin1 during *in vivo* tumorigenesis was investigated in the transgenic adenocarcinoma mouse prostate (TRAMP) mouse model of prostate cancer progression. As shown on Figure 6B, talin1 immunoreactivity was primarily detected among the glandular epithelial cells in the TRAMP prostates. Talin1 levels progressively increased with increasing age of TRAMP mice (6 - 27wks) [Fig. 6, panels (iii-vi)]. There was weak talin1 immunoreactivity in prostate tissue from wild-type (WT) control mice, while the intensity of talin1 staining was stronger in primary prostate tumors, with the

highest detected in liver metastases (Fig. 6 ii). Quantitative analysis revealed a 2-fold increase in talin1 expression in prostate tumors derived from 12wk TRAMP mice, compared to the 6wk old TRAMP prostates (Table 1). By 27 wks of age, upon time TRAMP mice exhibit a highly aggressive prostate tumor phenotype (grade 4.5-5), talin1 immunoreactivity increased dramatically (Fig. 6), a change that reached a statistical significance (<0.01, Table 1).

To determine whether talin1 might have a potential value for predicting human prostate cancer progression to metastastic disease, we conducted an immunohistochemical staining for talin1 in human prostate tissue specimens. Talin1 expression was analyzed in human prostate tissue specimens from normal, BPH, primary tumors (Gleason 6-9) and metastatic tumors (Table 2). Detection of immunoreactivity was followed by automated quantitative analysis to measure the cytoplasmic levels of talin1. A representative picture of normal prostate, BPH, primary prostate tumor and metastatic lesion to the lymph node is shown on Figure 7 (Panel A). Cytoplasmic talin1 was significantly higher in metastases than in primary tumors and both were significantly elevated compared to normal prostate tissue ($P<0.0001$, $P<0.0001$, respectively). These findings suggest that talin1 expression is positively associated with human prostate cancer progression to metastatic disease. Normal areas of prostate adjacent to tumor foci expressed lower talin1 levels compared to the remaining normal prostate tissue (Table 1). Talin1 expression detected in BPH specimens was comparable to those detected in normal prostate tissue.

DISCUSSION

The present study identifies talin1 as a novel regulator of prostate cancer cell invasion and metastatic potential, via its ability to enhance survival signals and confer anoikis resistance. Several key survival signaling pathways including AKT, FAK and Ras/Erk are activated by integrin adhesion and detachment from the ECM results in their inactivation[17]. Anoikis, (detachment from the ECM), results in activation of pro-apoptotic proteins and inhibition of anti-apoptotic proteins[22,23]. Our findings demonstrate that talin1 overexpression significantly enhanced the migration and invasion potential of human prostate cancer cells via an AKT-dependent mechanism. In contrast, loss of talin1 led to a diminished invasion potential and in vivo metastatic ability of prostate cancer cells. These results are in accord with a previous screening reporting that highly metastatic cells expressed significantly high levels of talin1 (>16 fold, out of 440 proteins screened) compared to less metastatic cells[24]. Interestingly enough, in primary prostate cancer cells, talin1 mRNA has been shown to be downregulated by androgens[25]. Taken together this evidence supports an indirect link between talin1 and prostate cancer metastasis and emergence to androgen-independence.

Overexpressing talin1 in prostate cancer cells led to activation of FAK/AKT signaling via both an ECM-dependent and -independent mechanism. Gaining strong support from evidence that AKT survival signaling is causally linked to anoikis resistance in detached cells[26,27], our data indicate that talin1 promotes prostate cancer cells to metastasize by enhancing their invasive properties and survival after detachment from the primary tumor site via activation of FAK and AKT signaling. This resonates with a

similar role assigned to another key focal adhesion protein, paxillin in different tumors. Indeed, overexpression of paxillin correlates with metastatic and invasion properties in hepatocellular carcinoma [28]. Recruitment of FAK and paxillin to β1 integrin promotes cancer cell migration through MAPK activation [29]. The present findings suggest that talin1 might not be causally involved in primary tumor development, but rather in promoting local invasion, as well as distant metastasis, via conferring resistance to anoikis. Such anoikis regulation by talin1, is not a selective advantage during tumor growth in an ECM-rich microenvironment; rather during the invasion through vasculature during metastasis, resistance to anoikis could predict a greater ability to form metastatic lesions. A similar functional contribution in strongly enhancing metastasis but not primary tumor growth, was demonstrated by the apoptotic suppressor of cytoskeleton-dependent death, Bcl-Xl during mammary carcinogenesis. [30]

Mechanistic dissection revealed that talin1 interferes with ILK-1 binding to integrin β3 subunit. ILK is a serine/threonine protein kinase, that interacts with cytoplasmic domain of β1-integrin and β3-integrin and has been functionally linked to integrin and Wnt signaling pathways[7,19,31]. Upon cell adhesion, ILK is transiently activated and directly phosphorylates PKB/AKT and glycogen synthase kinase-3 (GSK3)[6]; in contrast, inhibiting ILK in cancer cells inhibits AKT phosphorylation and cell survival; taken together these lines of evidence point to a potentially critical role for ILK in signaling anoikis resistance and cell survival mechanisms. Indeed, the present results indicate that talin1 loss partially abrogates ILK-1 binding to integrin β3, implicating ILK-1 as an intracellular effector of talin1 signaling, activated upstream of the AKT survival pathway. This *in vitro* evidence suggests that talin1 confers anoikis

resistance (non-adherent) and mediates direct ECM-epithelial interaction (adherent conditions). Based on these findings, we propose that such an effect of talin1 on anoikis might be responsible for the acquisition of the primary tumor cell invasive and metastatic properties leading to prostate cancer metastasis (Fig. 8). In this mechanistic scenario, under adherent conditions, talin1 facilitates integrin signaling and its link to the ECM. Talin1 binding to β integrin recruits the focal adhesion proteins ILK, FAK and SRC, towards activation of the downstream signals such as AKT and ERK. This signaling activation promotes cell survival, invasion and angiogenesis. Under non-adherent conditions, talin1 stimulates FAK and SRC independent of integrin signaling and confers resistance to anoikis, leading to metastatic spread of prostate cancer cells (Fig. 8). The concept derives strong support from our *in vivo* findings. Analysis of talin1 protein expression in the TRAMP model of prostate tumorigenesis, indeed demonstrated a positive correlation between talin1 immunoreactivity and prostate cancer progression to metastasis. A greater than 2-fold increase in talin-1 expression was detected in prostate tumors from 12wk TRAMP mice (compared to 6wk TRAMP); talin1 levels were further elevated with tumor progression to advanced metastatic disease (27wks) (Table 1).

Of major clinical relevance is immunostaining screening of talin1 in human prostate specimens indicating a significant increase in talin1 expression in primary tumors and metastatic prostate cancer, compared to BPH and normal prostate. The metastatic specimens exhibited significantly higher talin1 levels compared to primary prostate tumors, implicating an involvement of talin1 in the metastatic process. Talin1 expression was considerably higher in poorly differentiated prostate tumors (Gleason >8) compared to moderately differentiated (tumors Gleason 6/7). Moreover, there was an

inverse correlation between talin1 increased expression and E-cadherin loss in human prostate tumors and metastastic specimens (data not shown). These results support that talin1 may have diagnostic value in prostate cancer detection and clinical outcome. Ongoing studies focus on a correlation between talin1 expression with serum PSA levels, Gleason grade and patient (disease-free) survival in a large cohort of prostate cancer patients, which may define the value of talin1 as a cancer metastasis marker.

In summary, the evidence presented supports a function for talin1 in regulating prostate tumor cell invasion, and anoikis resistance towards metastasis. Future studies will pursue the generation of a conditional knockout mouse model of talin1, selectively targeting talin1 gene expression in prostate epithelial cells and its crossing with a transgenic mouse model of prostate cancer (since the homozygous talin1 knockout mice are embryonically lethal[11]). Ongoing efforts focus on characterizing talin 1 interactions with other binding partners such as paxillin, vinculin, and the impact of such interactions on the phosphorylation status of critical downstream signaling effectors in the context of integrin-related signal transduction. Further dissection of the contribution of talin1 to anoikis resistance mechanisms driving tumor and endothelial cell survival, may provide new signaling platforms for therapeutic targeting of metastatic prostate cancer.

MATERIALS AND METHODS

Cell Culture and Transfections: Human prostate cancer cell lines PC-3, DU-145, LNCAP, CWR-22, were obtained from the American Type Tissue Culture Collection (Rockville, MD) and cultured in RPMI-1640 (Invitrogen, Carlsbad, CA) containing 10% fetal bovine serum (Invitrogen) and antibiotics, PenicilinG/Streptomycin (50μg/ml). Human vascular endothelial cells (HUVEC) and Human Microvascular Brain Endothelial cells (HBMEC) were cultured in endothelial basal medium (EGM-2) (Cambrex, East Rutherford, New Jersey). Transfection was performed using Lipofectamin^{TM} 2000 reagent (Invitrogen, Carlsbad, CA) according to the manufacturer's protocol. PC-3 cells were transfected with pEGFP vector or GFP-Talin1 plasmids) and cloned under G418 selection (Geneticin, Gibco Brl, Grand Island, NY). For silencing talin1 expression in prostate cancer cells, the ShRNA talin1 vector (GIPZ ShRNAmir talin1) was obtained from Open Biosystems (Huntsville, AL). ShRNA talin1 DU-145 cells were selected using puromycin (a resistance marker) and individual clones were expanded.

Attachment Assay: Cells were seeded in six-well plates ($5x10^4$cells/well) coated with fibronectin (BD Biosciences Discovery Labware, Bedford, MA). Following a 10-min attachment period, attached cells were fixed with methanol (100%) and stored at 4°C in PBS for image analysis. Cells were counted in three x100 fields/well.

Migration Assay*:* Cell cultures (at 75% confluency) were subjected to wounding as previously described[32]. At 24 and 48hrs post-wounding cells migrating to the wounded areas were counted under the microscope.

Transendothelial Migration (TEM) Assay: Sterile (12mm diameter) glass coverslips were coated with Matrigel (Becton Dickson, Franklin Lakes, NJ). Coverslips were then seeded (at a density of $6.25x10^4$ HBMEC) to form a complete monolayer. Cells were allowed to adhere and spread on the Matrigel for 24hrs prior to initiation of the migration assay. PC-3 and DU-145 cells were resuspended in EGM-2MV (Cambrex) and added to the HBMEC monolayer ($8x10^3$cells/coverslip), for 12hrs. Cells were subsequently fixed in paraformaldehyde (2% in PBS) (10mins at room temperature) and washed with PBS. Nuclei were stained with DAPI Nucleic Acid Stain (Molecular Probes, Eugene, OR). Slides were visualized and examined under confocal microscopy.

Western Blot Analysis*:* Protein expression was determined by immunoblotting using the following specific antibodies: The human polyclonal rabbit talin1 antibody was generated and provided Dr. Richard McCann. The antibodies against FAK, AKT, phospho-Akt(Ser473), p44/42-MAP kinase, phospho p42/44-MAP kinase, SRC, Phosopho-SRC(Tyro416), GSK3-b, phospho-GSK3-b and ILK-1 were obtained from Cell Signaling Technology (Beverly, MA); The phospho-FAK(Y397) was obtained from Sigma (St. Louis, MO). Protein levels were normalized to α-actin expression, detected by using the α-actin antibody from Oncogene Research Products™ (La Jolla, CA). Cell lysates were prepared in RIPA buffer [150 mmol/l NaCl, 50 mmol/l Tris (pH 8.0), 0.5% deoxycholic acid, 1% NP-40 with 1 mmol/l phenyl methyl-sulfonyl fluoride]. Protein content was quantified using the bicinchoninic acid (BCA) protein assay kit (Pierce, Rockford, IL) and protein samples (30μg) were subjected to SDS-PAGE and transferred to Hybond-C membranes (Amersham Pharmacia Biotech, Piscataway, NJ). Membranes were blocked in 5% milk in TBS-T (TBS containing 0.05% Tween 20) (1 hr at room

temperature) and following incubation with the respective primary antibody (overnight at 4°C), membranes were exposed to species-specific horseradish peroxidase–labeled secondary antibodies. Signal detection was achieved with SuperSignal West Dura Extended Duration Substrate (Pierce) and visualized using a UVP Imaging System. Fold change in specific protein expression was determined on the basis of α-actin expression as a loading control.

Immunoprecipitation: DU-145 cells, ShVector control and ShTalin1 transfectants were lysed in RIPA buffer. Total protein concentration was quantified (as described above) and protein samples (100μg) were incubated overnight at 4°C with the specific antibody. Following incubation of lysates with Protein G Plus/Protein A agarose beads (30μl) for 3hrs at 4°C, beads were washed in RIPA buffer, subjected to SDS-PAGE analysis, and transferred to nitrocellulose membranes (Amersham Pharmacia).

AKT inhibitor: The AKT inhibitor; 1L6-Hydroxymethyl-chiro-inositol-2-(R)-2-O-methyl-3-O-octadecyl-sn-glycerocarbonate, was purchased from Calbiochem (Gibbstown, NJ). The concentration of inhibitor used was 10μM as previously reported [33].

Apoptosis Evaluation: Cells were harvested in EDTA buffer (0.5mM) and incubated in Hanks Balanced Salt Solution (HBSS) supplemented with 2% BSA and 0.01% sodium azide (30mins at 4°C). Cells were subsequently fixed in 4% (w/v) formaldehyde in PBS, and exposed to Annexin-V (R&D Systems, Minneapolis, MN) followed by FITC-conjugated secondary antibody. Analysis of Annexin V fluorescence was performed using flow cytometry (Partec, Munster, Germany).

Confocal Laser Scanning Microscopy: PC-3 prostate cells were cultured on four-chamber culture slides (BD Falcon, Bedford, MA). Cells were fixed in 4%

paraformaldehyde and permeabilized with 0.2% Triton X-100. Cells were exposed to the specific antibody, incubated with Alexa 546-conjugated goat anti-rabbit and mouse (Invitrogen), and were subsequently examined by confocal laser scanning microscopy (Leica Microsysterms, Wetzel, Germany) with constant intensity settings. Images were analyzed with Leica software (Leica Microsysterms).

Cell Cycle Arrest-Flow Cytometric Analysis: Cells were fixed with 70% ethanol (30mins at 4°C) and were subsequently stained with Propidium iodide (50µg/ml) containing 20µg/ml of RNase (30mins at room temperature). Cell cycle progression was analyzed via fluorescence-activated cell sorting (FACS) using the Partec Flow Max.

Anoikis Evaluation: Cells were plated on dishes coated with either fibronectin or the nonadhesive polyhydroxyethylmethacrylate (poly-HEMA) and incubated for 24hr. Cells undergoing apoptosis were detected using the Annexin V immunofluorescence approach and flow-cytometric analysis. Western blotting was used to determine the expression of key apoptosis regulators after overexpression and silencing of talin1 in prostate cancer cells.

***In Vivo* Experimental Metastasis Assay:** Human prostate cancer cells were injected ($2x10^6$ cells /80µl of PBS) in the tail vein of male nude mice (4–6 wks). After 5-weeks mice were sacrificed and the lungs and liver were surgically excised and examined for metastatic lesions under a dissecting microscope (40x).

TRAMP Transgenic Mouse Model: The TRAMP mice (C57BL/6J) are transgenic mice that express SV40T/t antigens under the prostate specific rat probasin promoter[34,35]. TRAMP transgenic males develop prostate adenocarcinoma in a manner resembling the clinical progression of human prostate cancer from intra-epithelial

neoplasia to androgen-independent metastatic tumors. Histological hematoxylin and eosin (H&E) sections of prostate tissues from TRAMP/+/+ male mice were evaluated by two independent investigators (S.S. and N.K.) to confirm the pathological grade. Wild-type male mice (C57BL/6) of comparable age groups (6-29wks) served as controls. The histopathological grading of prostatic tumors was conducted using a standard grading scale in TRAMP mice. Flat lesions and focal cell piling (grade 2.0-2.2) were observed in the majority of 12wks-old TRAMP mice (Table 1). In 20wk-27wk-old TRAMP mice, prostates exhibited focal cribriform lesions protruding into the lumen (grade 3-5), representing tumor progression to advanced disease.

Prostate serial sections from the normal wild type and the TRAMP tumors of increasing grade and metastatic lesions (5μm), were subjected to immunohistochemical analysis for talin1 using the talin1 polyclonal antibody (generously provided by Dr. McCann). Slides were examined under a Nikon fluorescence microscope (Nikon Inc., Melville, NY). Values were determined in a semiquantitative fashion, incorporating both the intensity of staining and the number of positively stained epithelial cells[36]. Briefly, the staining intensity (I) was graded as 0, absent; 1, weak; 2, moderate; or 3, strong. The proportion (P) of positive epithelial cells (0.0 to 1.0) with the staining intensity was recorded; A score for each histological grade (H) was determined as the product of intensity and proportion ($H = I \times P$).

Human Prostate Specimens: Human prostate tissue microarrays (TMAs), from patients with primary and metastatic prostate tumors were subjected to immuno-profiling for talin1 expression (subcontract with the Department of Pathology, University of Pittsburgh). Computer-image analysis was used to determine the level of talin1

expression in the prostate tissue specimens: 42 normal prostate; 101 normal areas surrounding malignant tissue; 56 BPH areas; 31 prostate primary tumors (Gleason Score range 6-9); and 74 metastatic lesions.

Statistical Analysis: One-way analysis of variance (ANOVA) was performed using the StatView statistical program to determine the statistical significance between values (*P* value less than 0.05). Tissue immunoreactivity was analyzed and interpreted according to previously published protocols[37].

ACKNOWLEDGEMENTS

This work was supported by an NIH R01 CA107575-06 grant (NK), a Markey Cancer Foundation Grant (NK) and an American Cancer Society IRG Grant (ROM). Shinichi Sakamoto is an American Urological Association Foundation Research Scholar. The authors acknowledge the expertise and help of Dr. Hong Pu with the animal experiments, Matthew Martelli for the initial in vitro experiments, Dr. Steven Schwarze for useful discussions and Lorie Howard for assistance with the manuscript submission process.

REFERENCES

1. Fornaro, M., Manes, T. & Languino, L.R. Integrins and prostate cancer metastases. *Cancer Metastasis Rev* **20**, 321-331 (2001).
2. McKenzie, S. & Kyprianou, N. Apoptosis evasion: the role of survival pathways in prostate cancer progression and therapeutic resistance. *J Cell Biochem* **97**, 18-32 (2006).
3. Frisch, S.M. & Francis, H. Disruption of epithelial cell-matrix interactions induces apoptosis. *The Journal of cell biology* **124**, 619-626 (1994).
4. Frisch, S.M. & Screaton, R.A. Anoikis mechanisms. *Current opinion in cell biology* **13**, 555-562 (2001).
5. Rennebeck, G., Martelli, M. & Kyprianou, N. Anoikis and survival connections in the tumor microenvironment: is there a role in prostate cancer metastasis? *Cancer research* **65**, 11230-11235 (2005).
6. Cieslik, K., Zembowicz, A., Tang, J.L. & Wu, K.K. Transcriptional regulation of endothelial nitric-oxide synthase by lysophosphatidylcholine. *The Journal of biological chemistry* **273**, 14885-14890 (1998).
7. Hannigan, G.E.*, et al.* Regulation of cell adhesion and anchorage-dependent growth by a new beta 1-integrin-linked protein kinase. *Nature* **379**, 91-96 (1996).
8. Radeva, G.*, et al.* Overexpression of the integrin-linked kinase promotes anchorage-independent cell cycle progression. *The Journal of biological chemistry* **272**, 13937-13944 (1997).
9. Calderwood, D.A. Integrin activation. *Journal of cell science* **117**, 657-666 (2004).
10. Giancotti, F.G. & Ruoslahti, E. Integrin signaling. *Science* **285**, 1028-1032 (1999).
11. Danen, E.H.J. Integrins and Development. Eurekah Bioscience Database, http://www.eurekah.com/index.php:. *Landes Bioscience, Austin* (2006).
12. Manes, T.*, et al.* Alpha(v)beta3 integrin expression up-regulates cdc2, which modulates cell migration. *The Journal of cell biology* **161**, 817-826 (2003).
13. Xing B, J.A., Lam SC. . Localization of an integrin binding site to the C terminus of talin *J Biol Chem.* **276**, 44373-44378 (2001).
14. Tanentzapf, G. & Brown, N.H. An interaction between integrin and the talin FERM domain mediates integrin activation but not linkage to the cytoskeleton. *Nature cell biology* **8**, 601-606 (2006).
15. Brown NH, G.S., Rickoll WL, Fessler LI, Prout M, White RA, Fristrom JW. . Talin is essential for integrin function in Drosophila. *Dev Cell.* **3**, 569-579 (2002).
16. Becam, I.E., Tanentzapf, G., Lepesant, J.A., Brown, N.H. & Huynh, J.R. Integrin-independent repression of cadherin transcription by talin during axis formation in Drosophila. *Nature cell biology* **7**, 510-516 (2005).
17. Bouchard V, D.M., Thibodeau S, Laquerre V, Fujita N, Tsuruo T, Beaulieu JF, Gauthier R, Vézina A, Villeneuve L, Vachon PH. Fak/Src signaling in human intestinal epithelial cell survival and anoikis: differentiation state-specific uncoupling with the PI3-K/Akt-1 and MEK/Erk pathways. *J Cell Physiol.* **212**, 717-728 (2007).
18. Calderwood, D.A.*, et al.* The phosphotyrosine binding-like domain of talin activates integrins. *The Journal of biological chemistry* **277**, 21749-21758 (2002).

19. Wu, C. & Dedhar, S. Integrin-linked kinase (ILK) and its interactors: a new paradigm for the coupling of extracellular matrix to actin cytoskeleton and signaling complexes. *The Journal of cell biology* **155**, 505-510 (2001).
20. Hannigan, G., Troussard, A.A. & Dedhar, S. Integrin-linked kinase: a cancer therapeutic target unique among its ILK. *Nature reviews* **5**, 51-63 (2005).
21. Horowitz, J.C.*, et al.* Combinatorial activation of FAK and AKT by transforming growth factor-beta1 confers an anoikis-resistant phenotype to myofibroblasts. *Cellular signalling* **19**, 761-771 (2007).
22. Miranti, C.K. & Brugge, J.S. Sensing the environment: a historical perspective on integrin signal transduction. *Nat Cell Biol* **4**, E83-90 (2002).
23. Reginato, M.J.*, et al.* Integrins and EGFR coordinately regulate the pro-apoptotic protein Bim to prevent anoikis. *Nat Cell Biol* **5**, 733-740 (2003).
24. Everley PA, K.J., Zetter BR, Gygi SP. . Quantitative cancer proteomics: stable isotope labeling with amino acids in cell culture (SILAC) as a tool for prostate cancer research. *Mol Cell Proteomics.* **3**, 729-735 (2004).
25. Betts AM, C.G., Neal DE, Robson CN. Paracrine regulation of talin mRNA expression by androgen in human prostate. *FEBS Lett.* **434**, 66-70 (1998).
26. Chang LC, H.C., Cheng CH, Chen BH, Chen HC. Differential effect of the focal adhesion kinase Y397F mutant on v-Src-stimulated cell invasion and tumor growth. *J Biomed Sci.* **12**, 571-585 (2005).
27. Irie, H.Y.*, et al.* Distinct roles of Akt1 and Akt2 in regulating cell migration and epithelial-mesenchymal transition. *J Cell Biol* **171**, 1023-1034 (2005).
28. Li HG, X.D., Shen XM, Li HH, Zeng H, Zeng YJ. Clinicopathological significance of expression of paxillin, syndecan-1 and EMMPRIN in hepatocellular carcinoma. *World J Gastroenterol.* **11**, 1445-1451 (2005).
29. Crowe DL, O.A. Recruitment of focal adhesion kinase and paxillin to beta1 integrin promotes cancer cell migration via mitogen activated protein kinase activation. *BMC Cancer.* **4**, 18 (2004).
30. Martin, S.S.*, et al.* A cytoskeleton-based functional genetic screen identifies Bcl-xL as an enhancer of metastasis, but not primary tumor growth. *Oncogene* **23**, 4641-4645 (2004).
31. Li, F., Liu, J., Mayne, R. & Wu, C. Identification and characterization of a mouse protein kinase that is highly homologous to human integrin-linked kinase. *Biochimica et biophysica acta* **1358**, 215-220 (1997).
32. Keledjian, K., Garrison, J.B. & Kyprianou, N. Doxazosin inhibits human vascular endothelial cell adhesion, migration, and invasion. *Journal of cellular biochemistry* **94**, 374-388 (2005).
33. Hu, Y.*, et al.* 3-(Hydroxymethyl)-bearing phosphatidylinositol ether lipid analogues and carbonate surrogates block PI3-K, Akt, and cancer cell growth. *Journal of medicinal chemistry* **43**, 3045-3051 (2000).
34. Gingrich JR, B.R., Foster BA, Greenberg NM. . Pathologic progression of autochthonous prostate cancer in the TRAMP model. *Prostate Cancer Prostatic Dis.* **2**, 70-75 (1999).
35. Greenberg NM, D.F., Finegold MJ, Medina D, Tilley WD, Aspinall JO, Cunha GR, Donjacour AA, Matusik RJ, Rosen JM. Prostate cancer in a transgenic mouse. *Proc Natl Acad Sci U S A.* **92**, 3439-3443 (1995).

36. Zeng, L., Rowland, R.G., Lele, S.M. & Kyprianou, N. Apoptosis incidence and protein expression of p53, TGF-beta receptor II, p27Kip1, and Smad4 in benign, premalignant, and malignant human prostate. *Human pathology* **35**, 290-297 (2004).
37. Camp, R.L., Chung, G.G. & Rimm, D.L. Automated subcellular localization and quantification of protein expression in tissue microarrays. *Nature medicine* **8**, 1323-1327 (2002).

FIGURE LEGENDS

Figure 1. Panel A, Generation of PC-3 Stable Transfectants Expressing GFP-talin1. pEGFP-talin1 and pEGFP vector stable transfectants were established in PC-3 cells selected under G418 Geneticin s a selection marker. The bands indicate GFP-talin1 (280kDa) and GFP-vector protein (28kDa) respectively. **Panel B,** pEGFP-talin1 mediated enhanced adhesion ability in PC-3 cells. The adhesion potential was comparatively analyzed in laminin or fibronectin-coated plates in PC-3 pEGFP vector control and PC-3 GFP talin1 cloned transfectants. **Panel C,** Talin1 expression enhances migration potential. PC-3 cells were subjected to wounding and migrating cells were counted under the microscope in three independent fields (40x)/well (3 wells/condition)(Panel D). Panels E, and F, Talin1 enhanced the migration potential through the endothelial monolayer. The transendothelial migration assay was performed using HBMECs, and either PC-3 GFP-vector or PC-3 GFP Talin1 expressing cells as described in "Materials and Methods".

Figure 2. Effect of Talin1 loss on Prostate Cancer Cell Migration and Invasion. **Panel A**, Talin1 ShRNA stable cell line in DU-145 cells. ShRNA talin1 stable cell line is established in DU145 cells. **Panel B,** ShRNA vector and ShRNA-talin1 transfectant cells were comparatively analyzed for their adhesion potential as described above. **Panel C,** Talin1 silencing reduces DU-145 cell migration ability. Cells were subjected to wounding and migration potential was evaluated; the number of migrating cells was counted under the microscope in three independent fields (40x) per well (3 wells/condition) (**Panel D**). **Panel E,** Loss of talin1 inhibits prostate tumor cell invasion.

Transendothelial migration assay were conducted using HBMEC (human brain microvascular endothelial cell) DU-145 vector and ShRNA Talin1 stable cell line. The number of invading cells (red) was determined under confocal microscopy (**Panel F**). Blue represents DAPI nuclear staining.

Figure 3. Talin1 Mediates ECM-dependent Activation of FAK/AKT Pathway.

Panel A, pEGFP-talin1 and vector-transfected PC-3 cells were allowed to adhere on either collagen or fibronectin plates. After 6hrs, cells are collected and subjected to western blot analysis. Levels of phosphorylated AKT (Ser473), FAK(Y397) and MAPK proteins as wells as total protein were detected using respective antibodies. **Panel B,**. Expression of p-FAK, p-AKT and p-MAPK pEGFP-talin1 and vector-transfected PC-3 cells (on fibronectin), were examined using specific antibody with Alexa 546 fluorescence (Red). Nuclei were stained with DAPI (Blue). (x400 magnification). **Panel C**, Phosphorylation of AKT (Ser473), FAK(Y397) and MAPK was analyzed after adherence to fibronectin as indicated (3-24hr). **Panel D,** Quantification of phosphorylation status of AKT (Ser473), FAK(Y397) and MAPK was determined by densitometry**. Panel E**, ShTalin1 DU-145 cells were subjected to immunoprecipitation using the integrin β3 antibody. Talin1, total FAK and SRC binding was detected using the respective antibodies. **Panel F**, Cells (as above) were subjected to immunoprecipitation using monocolonal integrin β3 antibody or polycolonal ILK-1 antibody. Binding of ILK-1 or integrin β3 was determined using the respective antibodies.

Figure 4. Talin1 Mediates Anoikis Resistance. Panel A, pEGFP-talin1 and vector PC-3 cells were kept in suspension conditions for 24hr using Poly-HEMA coated plates. Apoptosis was determined by Annexin-V immunofluorescence and the % of Annexin-V positive cells over the total number of cells are shown on the barograph. **Panel B,** After 24hr of cell suspension, cells are lysed and subjected to Western blot analysis. Phosphorylation of AKT (Ser473), FAK (Y397) and p42/44MAPK together with total proteins were detected using respective antibodies. **Panel C**, Phosphorylation of AKT (Ser473), FAK (Y397) and SRC and total protein expression was studied during various time points (3-24hr). **Panel D,** The phosphorylation status of AKT (Ser473), FAK (Y397) and SRC was analyzed by densitometry. **Panel E,** Phosphorylation of GSK3b and total GSK3-b and cleaved caspase-3 were determined during the same time course (3-24hr). The fold-changes relative to vector control are shown on Panel F.

Figure 5. Consequences of AKT Inhibion on Adhesion, Migration and Invasion of Talin1 Overexpressing Prostate Cancer Cells. Panel A, The impact of AKT signaling inhibition on the adhesion ability of GFP-talin1 stable PC-3 tranfectants to collagen, laminin or fibronectin coated-plates was determined as described in "Materials and Methods". **Panel B**, Prostate cancer cells were subjected to wounding and migrating cells (GFP-talin1 or GFP vector PC-3 cells) were evaluated at 24 and 48hr post-wounding, in the presence or absence of AKT inhibition. Three independent fields/well were counted (40x). **Panel C,** Transendothelial migration assay was conducted using HBMEC under conditions of AKT inhibition. The green color indicates migrating prostate cancer cells, the blue color indicates the nuclear DAPI staining**.**

Figure 6. Panel A, Talin1 Loss Suppresses Prostate Cancer Cell Metastasis. Nude mice were injected with prostate cancer cells, DU-145 ShVector, n=6 and DU-145 shRNA talin1, n=5, ($2x10^6$/mouse) in the tail vein. Five (5) weeks post-inoculation, the lungs were surgically dissected and metastastic lesions were evaluated. Silencing talin 1 resulted in a significantly reduced number of metastatic lesions to the lungs (P =0.028).

Panel B, Talin1 Immunostaining in TRAMP Mouse Model of Prostate Adenocarcinoma Progression. Talin1 immunreactivity was analyzed in paraffin-embedded prostate tissue specimens from TRAMP mice and control age-matched mice (6-27 wks). Pathological grading of the tumors was performed as described in "Materials and Methods". A strong immunoreactivity for talin1 was detected in prostate tumors derived from both 19wk and 27wk TRAMP mice, subpanels (iv) and (v), respectively. Sub-panel (ii) represents a metastatic lesion to the liver in a TRAMP mouse (27wks).

Table 1. Expression of Talin1 in Prostate Tumors from TRAMP Mice. The intensity of IHC staining (H) was calculated by P=Percentage of staining x I intensity (1-3). The numerical data reveal a positive correlation between increasing tumor grade and increased talin expression. Talin1 expression was significantly increased prostate tumor progression to metastasis. (*) and (**) indicates statistical difference at p value<0.05 and <0.01, respectively, compared to specimens from wild-type control mice.

Figure 7. Expression of Talin1 in Human Prostate Tissue. Talin1 immunreactivity was analyzed in paraffin-embedded prostate tissue specimens from human prostate cancer patients as described in "Materials and Methods". A

representative image for talin1 immunoreactivity is shown in each developmental stage, including the normal prostate (i); BPH (ii); Prostate Primary Tumor (iii); Metastatic Prostate Cancer (iv).

Table 2. Quantitative Evaluation of Talin1 Immunostaining in Human Prostate Tissue. Computer-image analysis was used to determine the level of talin1 expression in the prostate tissue specimens. Specimens included normal prostate, normal tissue adjacent to tumor foci, benign prostate hyperplasia, BPH; primary prostate tumor and lymph node metastasis. (*) and (**) indicate statistical difference at p value<0.05 and <0.01, respectively, compared to normal prostate.

Table 3. Association of Talin1 Expression and Gleason Score. Primary prostate cancer specimens were classified as moderately (Gleason 6/7) and poorly differentiated tumors (Gleason >8; 8, 9, 8/9) and talin1 expression values were comparatively evaluated. (*) and (**) indicate statistical differences at p-value<0.05 and p<0.01, respectively, compared to moderately differentiated tumors (Gleason 6/7).

Figure 8. Proposed Talin1 Signaling in Cancer Cells. Under adherent conditions, talin1 facilitates integrin signaling to the ECM. Talin1 binding to β integrin recruits the focal adhesion proteins ILK, FAK and SRC, towards acivtation of the downstream signaling. Subsequent activation of downstream AKT and ERK signals, promotes angiogenesis, cell cycle progression, cell survival and apoptosis resistance. Under non-adherent conditions, talin1 stimulates FAK/SRC and ILK-1/GSK3b related signals independent of integrin signaling and mediates anoikis resistance.

Figure 1

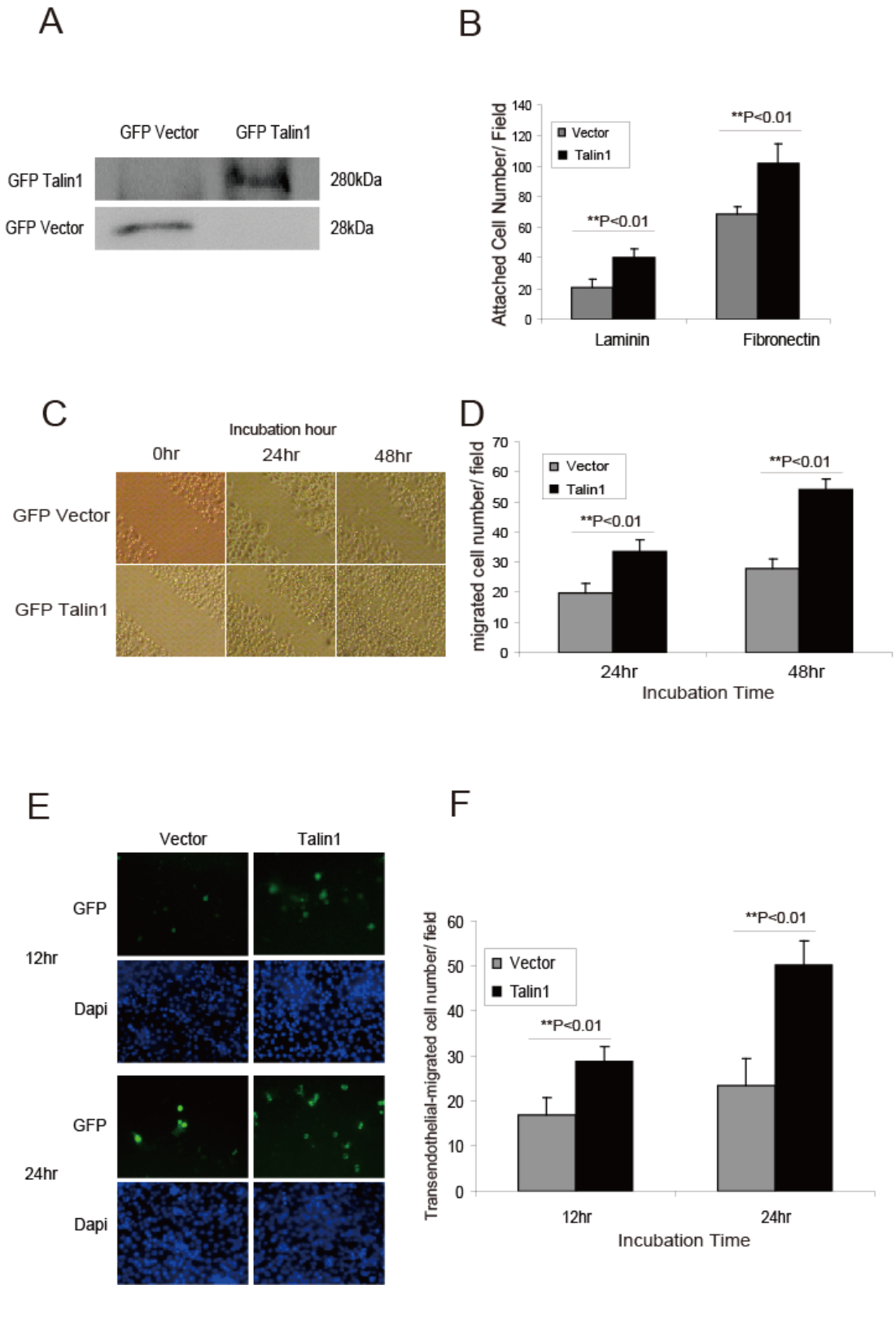

Figure 2

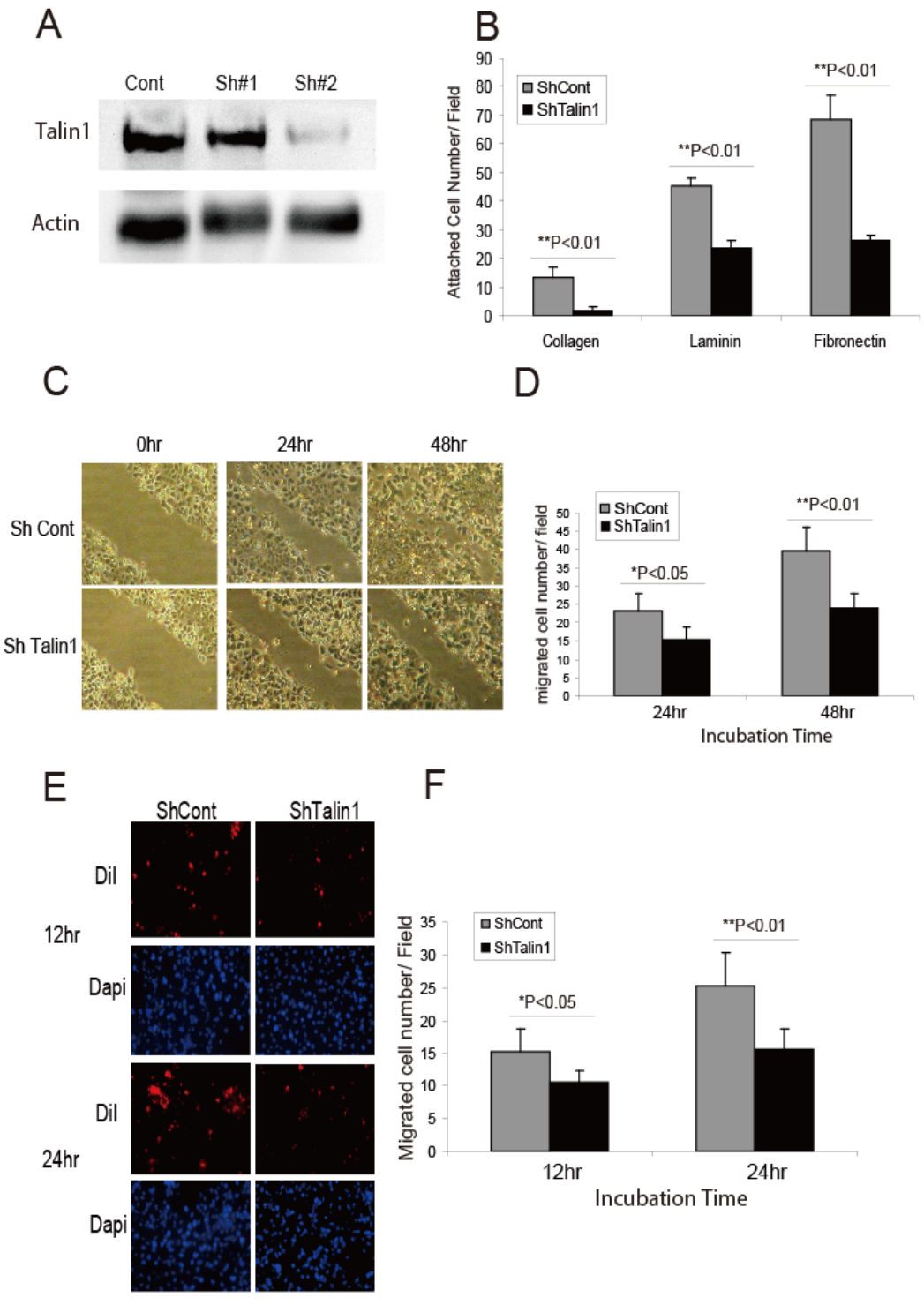

Figure 3

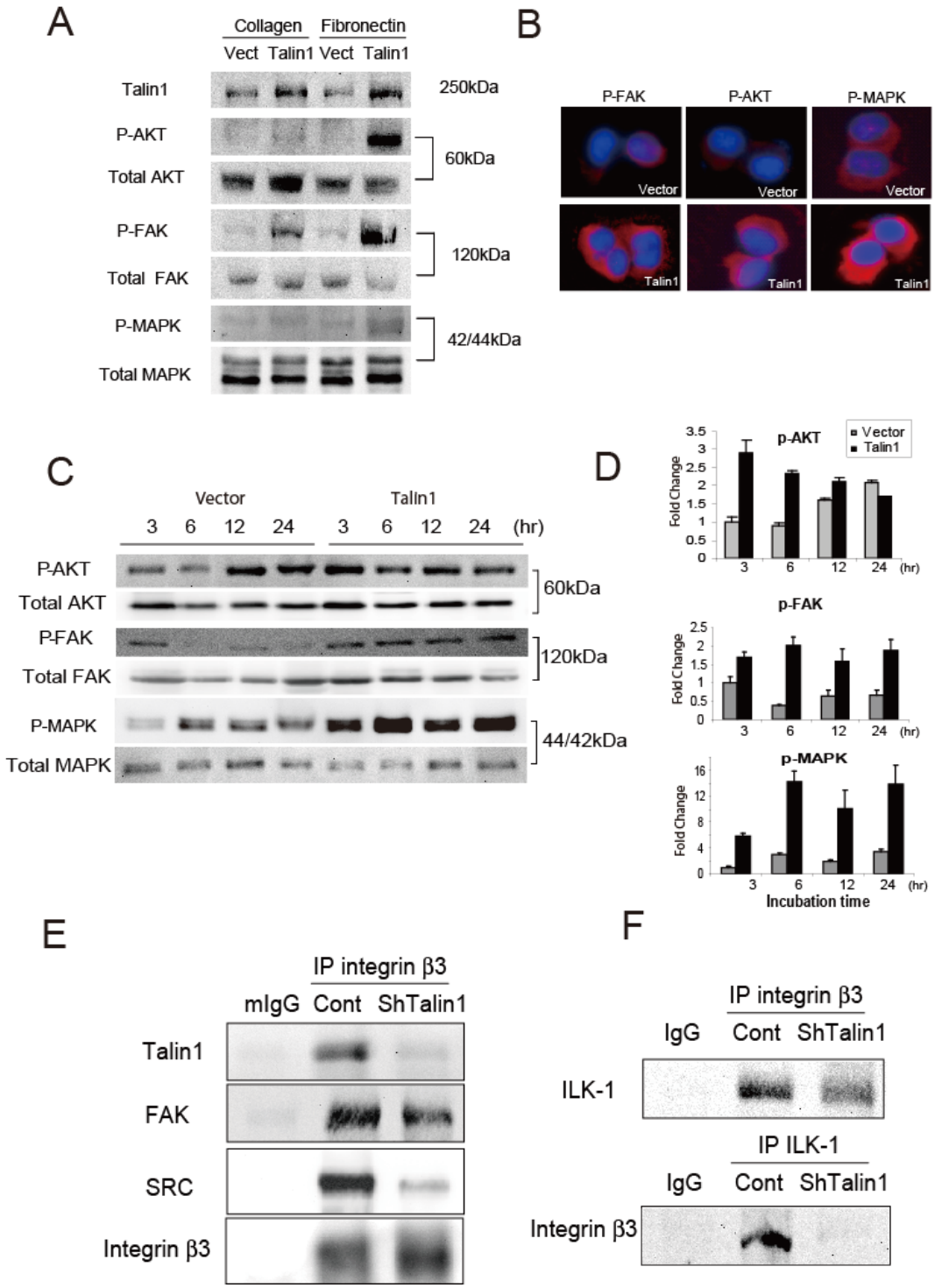

Figure 4

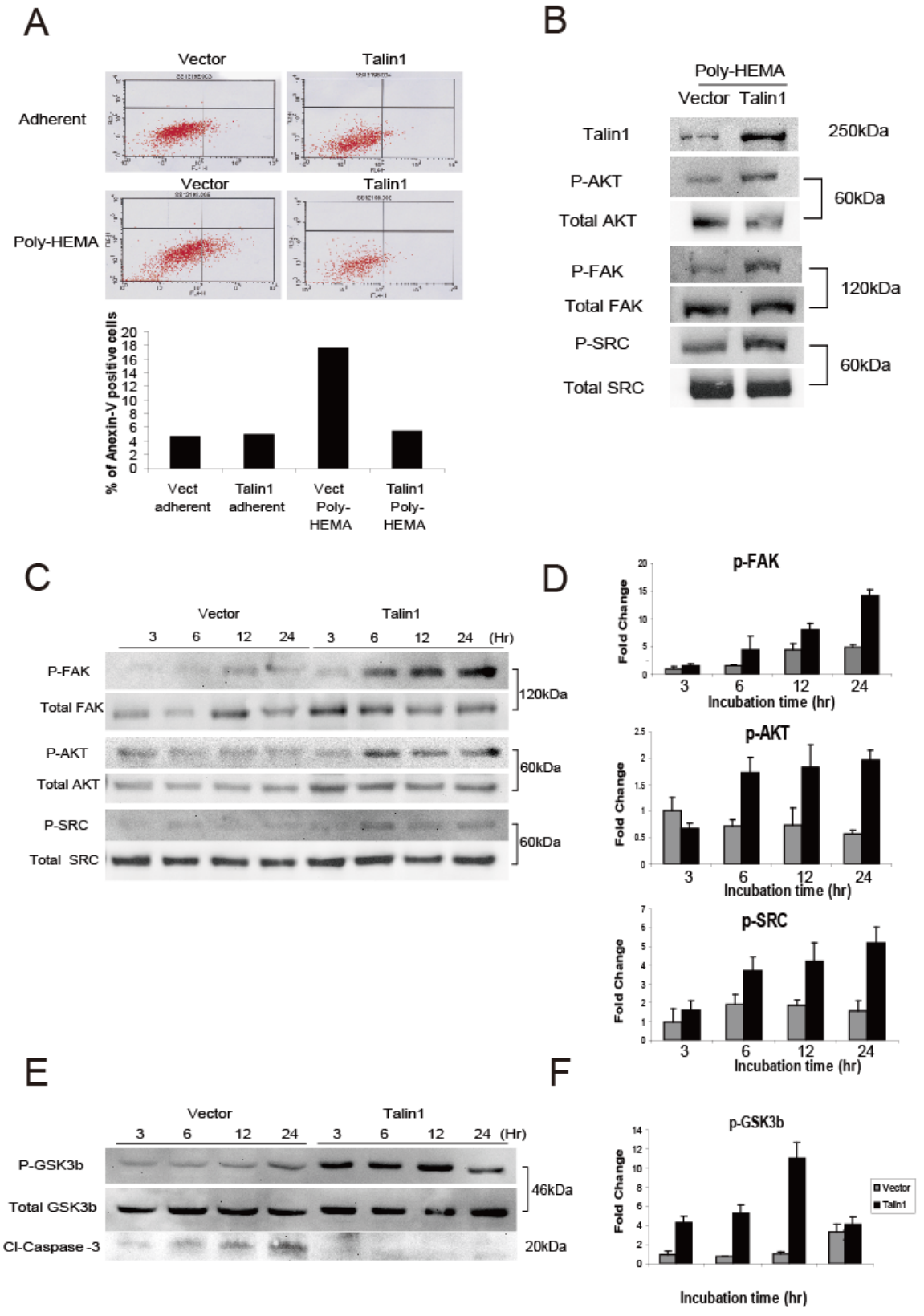

Figure 5

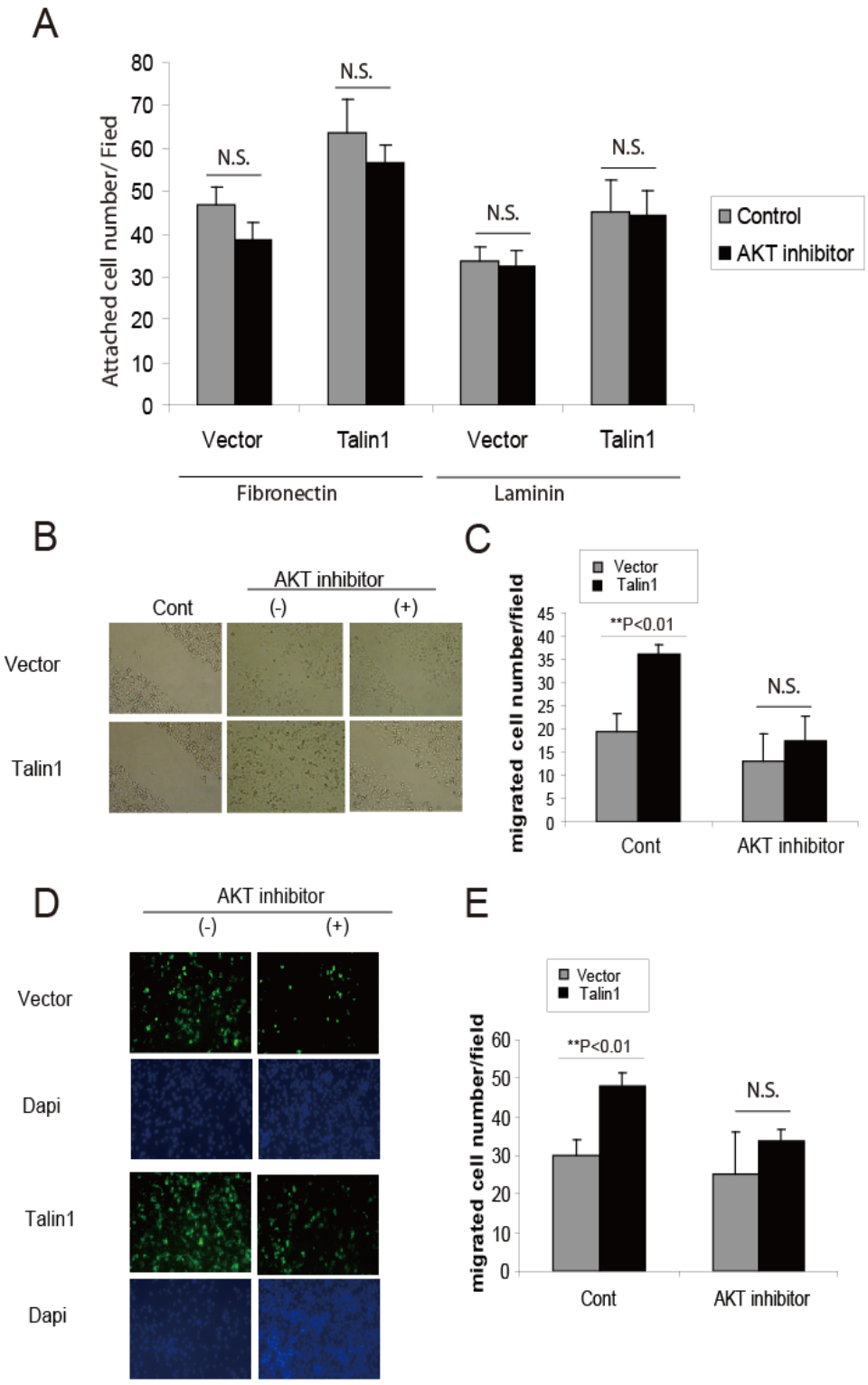

Figure 6

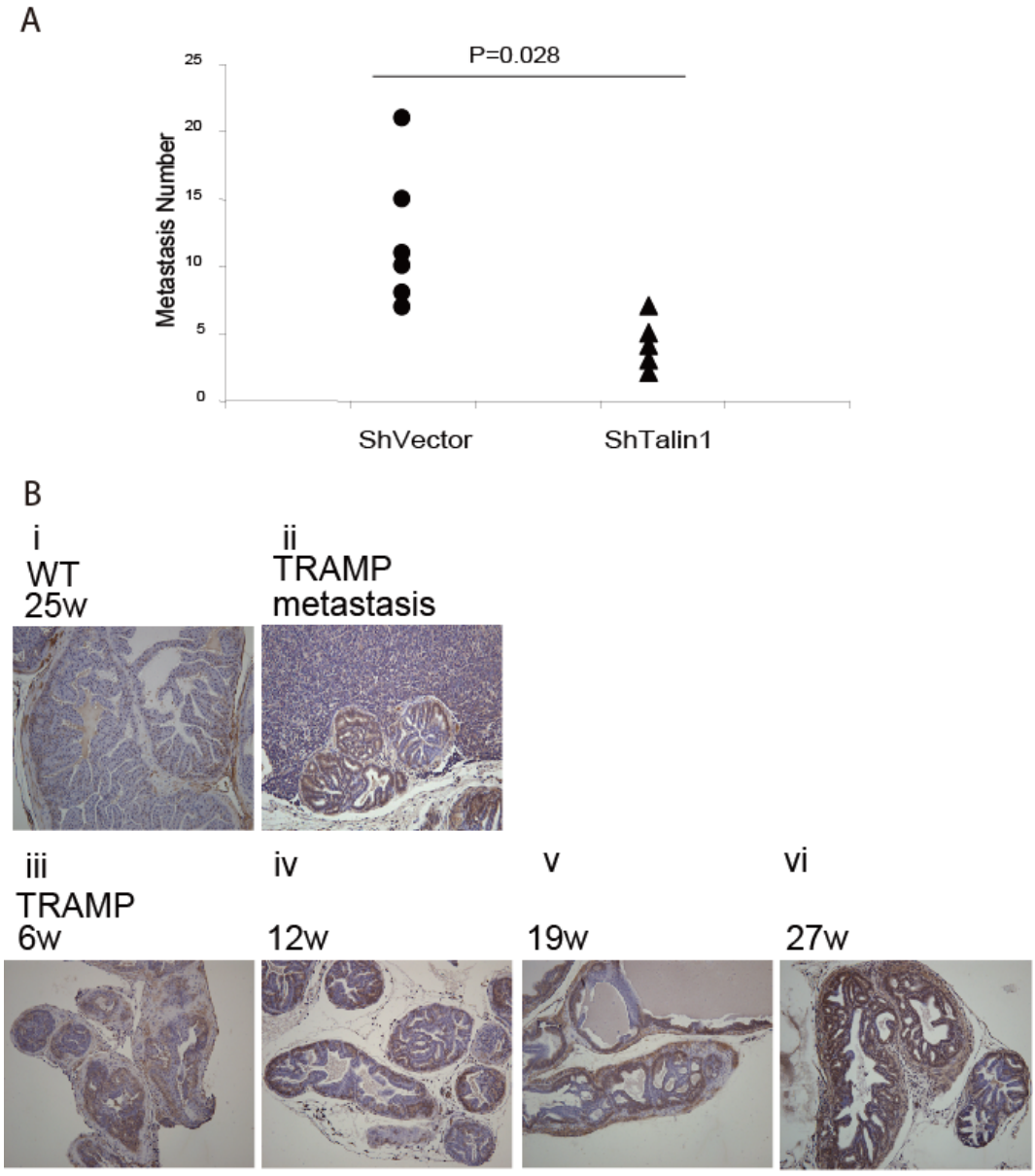

Table 1

Mice	Age	Tumor Grade	Talin1 level(H=Pxl)	P-value
Wild Type	25w	normal	0.48 ± 0.2	
	6w	normal	0.57 ± 0.3	0.638
	12w	2.2	1.31 ± 0.6	*0.078
TRAMP	19w	3.7	1.78 ± 0.6	*0.018
	27w	4.7	2.41 ± 0.4	**0.0019
	Metastasis	(-)	2.29 ± 0.2	**0.00012

Figure 7

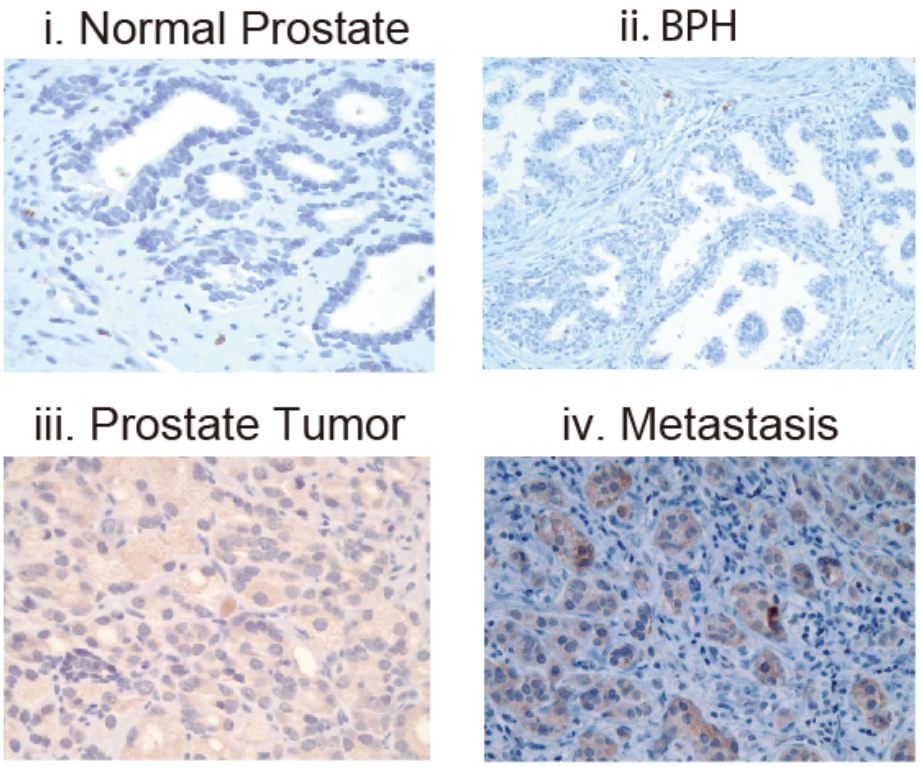

Table 2 Quantitative analysis of talin1 expression in human prostate tissue

Specimen	(n)	Intensity	P-value
Normal	(42)	155.4 ± 5.3	
Adjacent	(101)	150.2 ± 8.3	*0.017
BPH	(56)	155.2 ± 6.3	0.319
Primary Tumor	(34)	162.2 ± 7.8	**0.00028
Metastasis	(74)	167.3 ± 7.9	**0.0000009

Table 3 Talin1 expression in primary prostate tumor

Tumor Grade	(n)	Intensity	P-value
Gleason 6/7	(15)	154.2 ± 8.7	
Gleason 8	(9)	163.0 ± 10.3	*0.0327
Gleason 9	(10)	167.1 ± 4.5	**0.0005
Gleason 8/9	(19)	164.9 ± 8.2	**0.0009

Figure 8

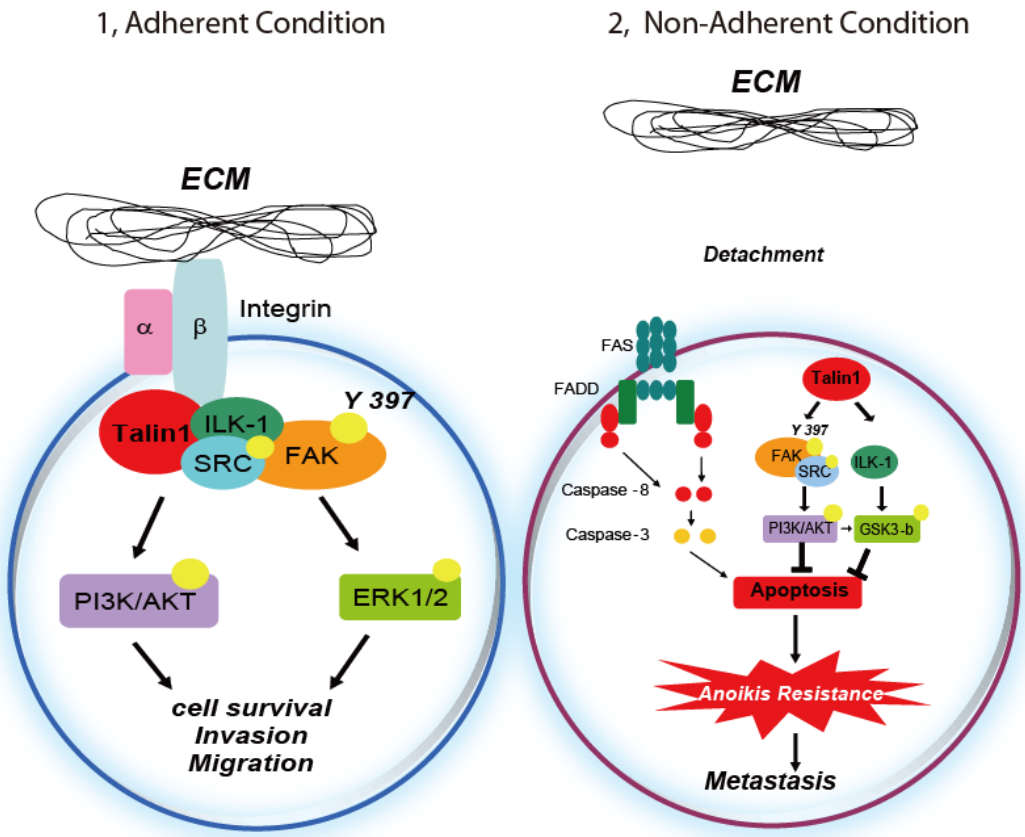

Supplementary 1

A

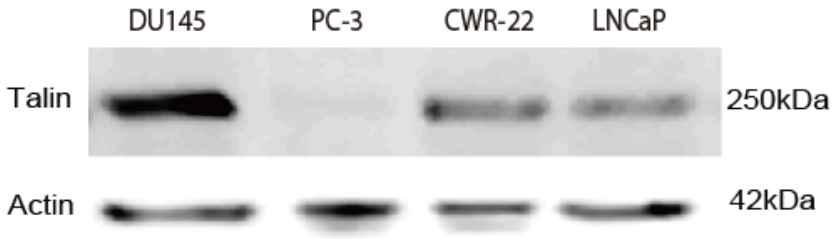

B

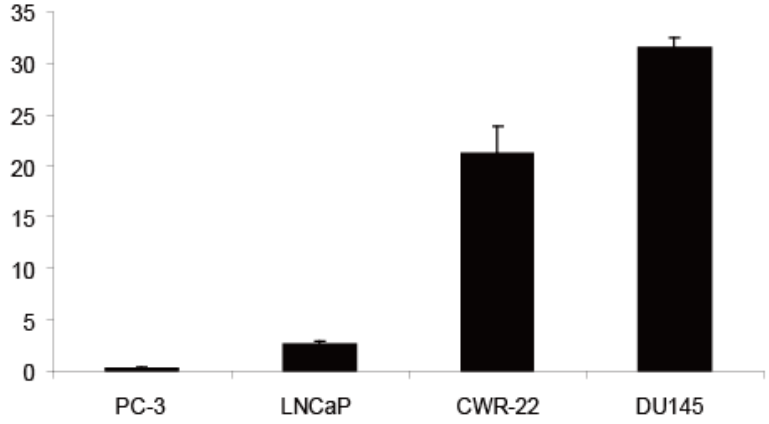

Supplementary 1: Panel A, **Expression of Talin1 in Human Prostate Cancer Cell Lines.** Western blot analysis of talin1 basal levels of expression in various human prostate cancer cell lines as shown. Actin expression was used as a loading control. Cell lysates were subjected to SDS page and detected with the respective specific antibody. **Panel B, mRNA expression profiling.** RNA samples from the various human prostate tumor epithelial cells were subjected to reverse transcription, and subsequent PCR using talin1 and 18S primers as described in "Materials and Methods". Talin1 mRNA expression was normalized to 18S expression.

Supplementary 2

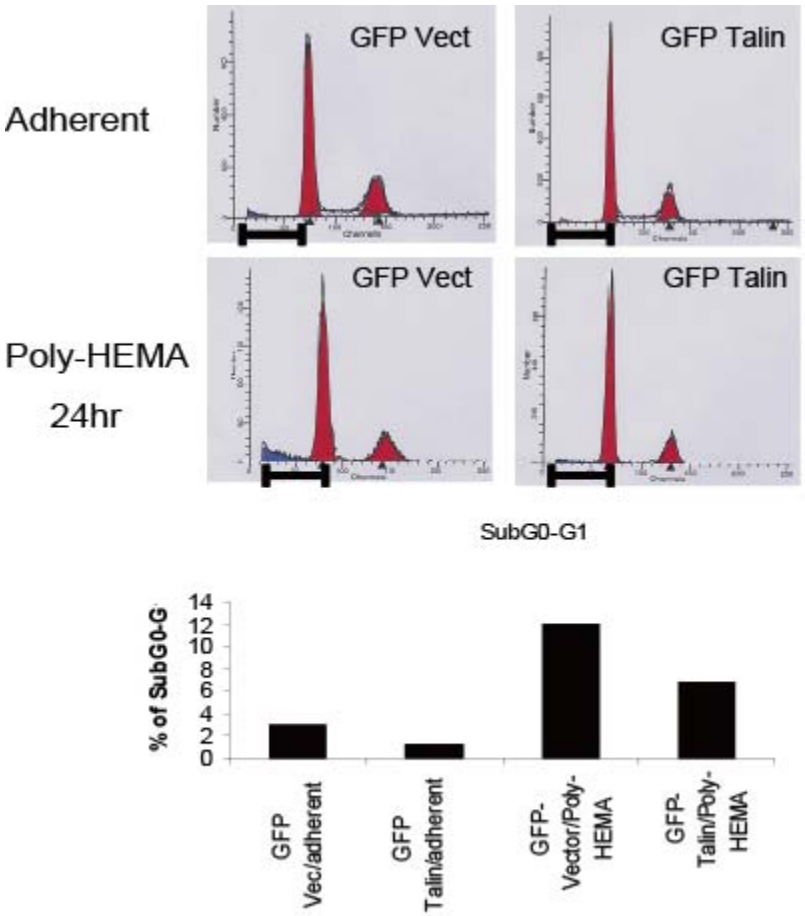

Supplementary 2: Effect of **Talin1 on G0-G1 Cell Population under Non-adherent Conditions.** GFP-Talin1 and GFP-vector transfected cells were incubated in non-adherent poly-HEMA conditions for 24hr and subjected to cell cycle analysis using PI staining through Flow Cytometry. The sub G0-G1 populations are shown on Panel A**.** Panel B indicates the quantitative analysis of SubG0-G1 population.